

NCAR's contribution to
**Improved tropospheric delay measurement
and precision orbit determination for satellite
ocean altimetry.**

a JPL/NCAR project,

Yoaz Bar-Sever, Principal Investigator,
Francois Vandenberghe, Bruce Haines, Steve Keihm and Charles Naudet
Co-investigators

Francois Vandenberghe and Yong-Run Guo

*National Center for Atmospheric Research
PO Box 3000, Boulder CO 80307-3000*

Progress Report

December 2000

1.0 Introduction

Satellite Oceanic altimetry measurement techniques strongly rely on Global Positioning System (GPS) technology. GPS receivers are used on board altimetric satellites to provide rapid orbit determination capabilities and on the ground where downward transmissions are used to calibrate the on-board altimetric radiometers. The calibration procedure aims at estimating from GPS transmission the phase delay due to the presence of water vapor structures in the troposphere, i.e. the low part from atmosphere (0 to 10/13km). The removal of these tropospheric delays in altimetric signals allows for height measurements (Haines and Bar-Sever 1998).

Accurate estimate of GPS tropospheric delays are, therefore, crucial for accurate ocean altimetry. Typical tropospheric phase delays are of the order of tens of centimeters and current GPS data processing techniques can provide estimates of tropospheric delay with millimeters accuracy using ancillary information of surface pressure and temperature. There are, however, ample evidence that such low-order techniques do not capture all the water vapor structures existing in the troposphere. For instance, post-fit phases of residuals from precise point positioning at a given site display a cosecant dependence on the GPS satellite elevation angle (Zumberge *et al.* 1997); indicating, thus, that not all the signal has been extracted during the fitting. These indications have been confirmed in studies using other techniques such as double differentiation and/or water vapor radiometer as validation instruments (Ware *et al.* 1997). Unfortunately, those residuals also contain noise and the extraction of additional tropospheric information is a very challenging problem.

This project aims at developing new techniques for filtering post-fit residuals. For that purpose, a GPS receiver and a water vapor (WV) radiometer have been set up in Lamont, Oklahoma. Lamont is in the middle of the Cloud and Radiation Test Bed (CART) of the Atmospheric Radiative Measurement (ARM) program. ARM is the largest world global change program supported by the Department of Energy. The program focus on obtaining field measurements and developing models to better understand the processes that control solar and thermal infrared radiative transfer in the atmosphere (especially in clouds) and at the earth's surface. There are three different measurements sites within the ARM program: the North Slope of Alaska site, the Tropical Wester Pacific site and the Souther Great Plains (SGP) site. The SGP area was the first field measurement site established by the ARM Program. The site consists of *in situ* and remote-sensing instrument clusters arrayed across approximately 55,000 square miles in north-central Oklahoma and south-central Kansas, see details at <http://www.arm.gov>. Within the SGP, the CART

site has an unique experimental setup with an extensive selection of weather instruments (balloon-borne sounding system, raingauges, eddy correlation system, Belfort Laser, Ceilometer, Micropulse lidar, millimeter-wavelength cloud radar, whole sky imager, etc.) which can be advantageously used to support or to validate various experiments with new instruments such as GPS receivers. In particular, the facility provides an unique opportunity to study and asses GPS receiver's performances in two important areas that have received little attention in the past, namely, under cloudy conditions and during rain. Cloud water and rain are generally assumed to be of the order of millimeter and to have a negligible impact on tropospheric delay. However, preliminary studies suggest that, cloud water and rain contribution can be of several centimeters at the center of thunderstorm supercell.

Both instruments the GPS receiver and the WV radiometer are able to track a GPS satellite as it rise and set in the sky and are sensible to the water vapor present along the satellite line of sight (LOS) transmission. In this project, the interest focus on GPS technology and the WV radiometer is used as comparison and validation instrument. At low elevation, however, WV radiometer's transmissions suffer from ground effects and cannot be used, while, in theory, GPS transmission are still possible to negative elevation angles. For those low angles, other validation techniques are required, these techniques include ray-tracing on atmospheric refractivity fields produced by a numerical weather prediction (NWP) model. The project, indeed, included the use of a NWP model for several purposes:

- i) To help to identify interesting meteorological situations.
- ii) To provide the ancillary information (surface pressure and temperature) at the Lamont location for tropospheric delay retrieval from GPS line of sight phase delay measurement
- iii) To simulate GPS LOS propagations at low elevation angle.

The purpose of this report is to describe the different numerical experiments carried out during the project. These experiments have been performed at NCAR with the fifth generation of the Penn State/NCAR Mesocale Model. The model set-up and a description of the simulations are provided in section 2. The ray-tracing technique and the simulated LOS tropospheric phase delays are presented in section 3. We sum up in section 4.

2.0 Numerical Simulations

The Penn State/NCAR mesoscale model (MM5 Version 3) has been used to simulate the meteorological conditions over Lamont (36.60North

97.49W and 287m elevation) for summer 1999. Because tropospheric water vapor can vary a lot on short time and space scale, very high resolution simulations were required. We use for that purpose three embedded domains with a spacial resolutions of 30km (D1), 10km (D2) and 3.3km (D3). See Figure 1 for the domain configuration. A fourth domain (D4) at 1.1 km was initially created, but couldn't be used because of its too high computational cost in terms of both simulation and ray-tracing.

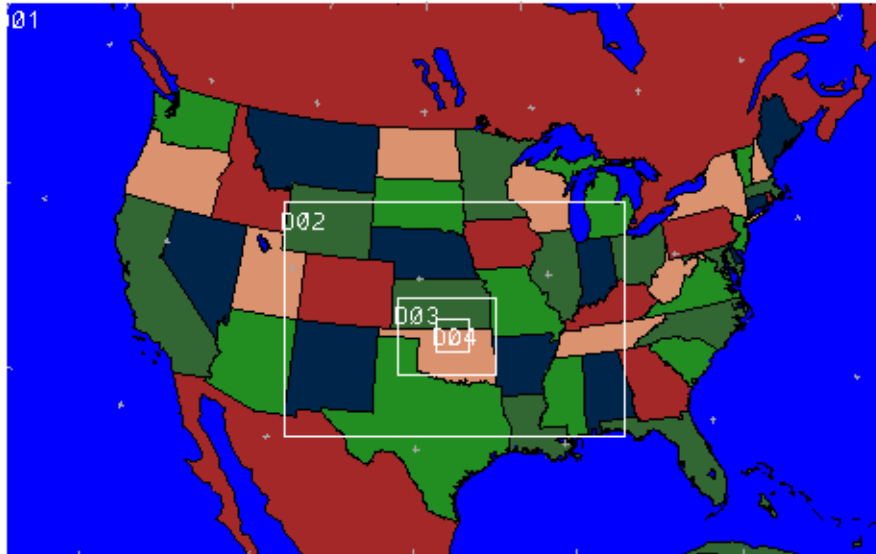


Figure 1:
MM5 domains configuration,
the resolutions for the domains are 30km (D1), 10km (D2), 3.3km (D3), 1.1km (D4).

On each domain, 12h forecasts initiated at 00z and 12z were performed daily for the whole month of July 1999. Outputs from the National Center for Environmental Predictions (NCEP) regional (Eta) model (Rogers *et al.* 1995) provided the initial and boundary conditions for domain D1, then output from domain D1, provided the initial and boundary conditions for domain D2 and son on. Domain D1 was run independently in real-time while boundaries conditions for domain D2 were saved every 6 hours. Simulation on domains D2 and D3 were simultaneous and nested, i.e. at every time step domains D2 and D3 exchange data through boundaries of domain D3.

Because the input fields from the Eta model are already analyzed at 00z and 12z at NCEP, they already include all the observational information available at that time on the Global Telecommunication System network from the US continental observational network and meteorological satellites. Therefore, in

the absence of additional mesoscale observations (local data were not used in this first experiment), there is no need to repeat these analyses at the mesoscale. The physical parametrization were the same for the three domains, they included the MRF Planetary Boundary Layer scheme, the Kain Fristch convective parametrization, the mixed phase microphysics (Reisner 1) and the cloud radiation (Grell *et al.* 1994).

For the three domains, forecasts were outputted every 1h and put on the web. Animation of the 3h rain accumulation, horizontal and zonal relative humidity, temperature and potential vorticity can be consulted at: <http://www.mmm.ucar.edu/individual/vandenberghe/lamont.html>. MM5 simulations showed a very strong precipitation events over Lamont on July 10, 1999 at 09z with a 3h accumulation rain of 35mm. However, July 16th and 17th 1999 were selected because a good agreement was found between GPS and WVR data. The precipitable water, i.e. the total content of water vapor in the atmospheric column (see section 3 for its exact definition), at 18z (1:00pm local time) on July 16 and 17, 1999 is shown on Figures 2 and 3. As we can see, precipitable water exhibits very fine scale spacial structures.

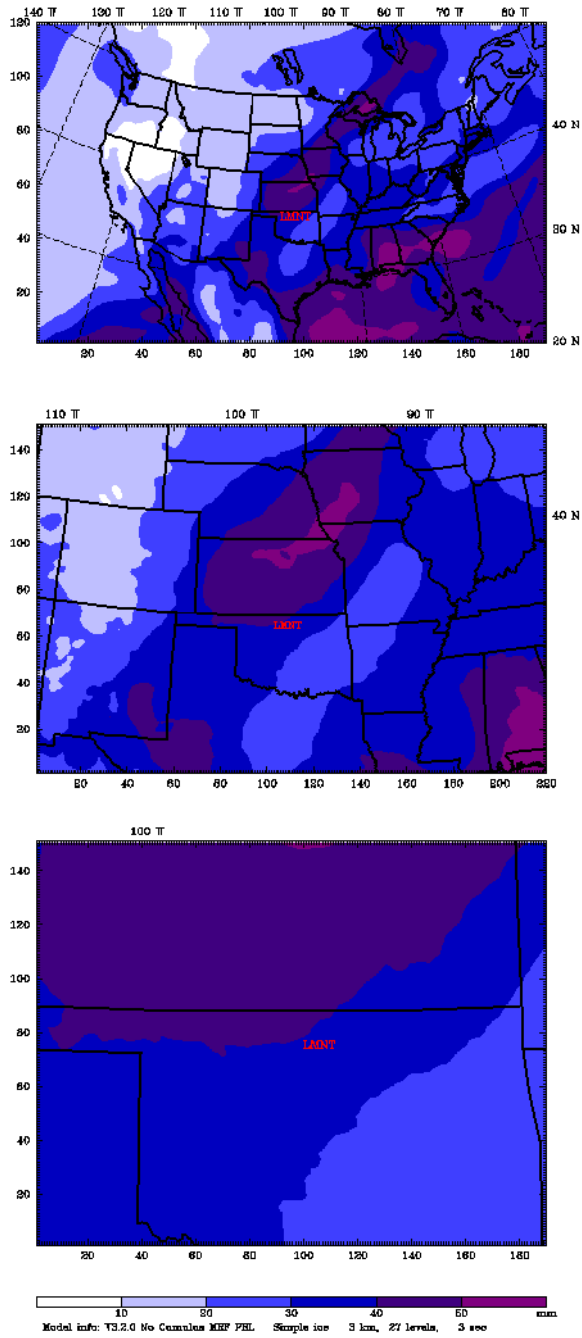


Figure 2:
6h forecast of precipitable water for the three domains
on July 16, 1999 at 18z (1:00pm local time).

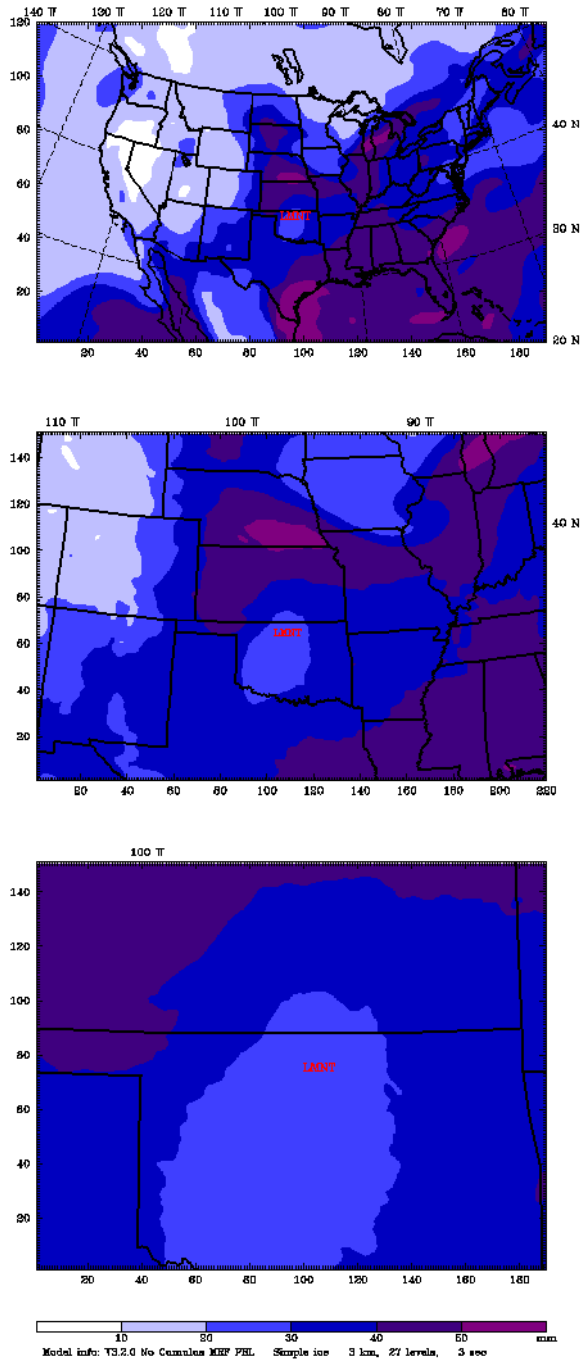


Figure 3:
6h forecast of precipitable water for the three domains
on July 17, 1999 at 18z (1:00pm local time).

3.0 Ray tracing

3.1 Definitions

Tropospheric delays in GPS downward transmissions are caused by the presence in the low atmosphere of refractivity gradients, usually due to non homogeneities in the water vapor field. These gradients result in a bending of the signal path and in a delay in the phase reception (compared to a transmission in the vacuum). The ray-tracing technique consists in the simulation of the transmission of the GPS electromagnetic signals by numerically solving the so-called ray equation (Kravtsov and Orlov 1990) given by:

$$\frac{d^2 \vec{r}}{d\tau^2} = n \vec{\nabla} n$$

$$d\tau = \frac{ds}{n}$$

Where \mathbf{r} is the position of the point on the ray path, s is the curvilinear coordinates of the ray and n is the refractivity index.

To numerically solve the ray-equation, we need to be able to compute the value of the refractivity index n at any location. This is made possible by pointwise interpolation of the 3-Dimensional refractivity index field provided by the NWP model. This gridded field is computed from the normal output fields: pressure (P), temperature (T) and water vapor pressure (e) using the following empirical relation (Bevis et al. 1992):

$$n = 1 + 10^{-6} \times 77.6 \frac{P}{T} + 3.73 \times 10^{-1} \frac{e}{T^2}$$

Once the ray-equation integrated; the phase delay, i.e. the excess of phase due to the presence of the atmosphere is obtained by integration along the ray path of the refractivity N , i.e. the part of the refractivity index accounting for the pressure, temperature and water vapor. The refractivity is defined from the refractivity index by the relation:

$$N = 10^6 \times (n - 1) = \underbrace{77.6 \frac{P}{T}}_{N_{dry}} + \underbrace{3.7310^5 \frac{e}{T^2}}_{N_{wet}}$$

To distinguish the effects due to water vapor only, it is convenient, as it is done in the above equation, to break down the refractivity N into the sum of a so-called dry refractivity N_{dry} and wet refractivity N_{wet} . Note that the term dry refractivity also contains the water vapor effects through the pressure, so the term dry delay is not fully appropriate. The terminology “hydrostatic delay” is sometimes preferred. However, this is convenient name to differentiate the effects caused water vapor only.

The total delay is obtained by integration of the refractivity along the ray path:

$$TD = \underbrace{\int_S N_{dry} ds}_{D_{dry}} + \underbrace{\int_S N_{wet} ds}_{D_{wet}}$$

Typically D_{dry} varies from 1m to 20m and D_{wet} varies from 10cm to 2m, with minimal values for vertical transmission, i.e. when the satellite is at the zenith and maximal values for horizontal transmission, i.e. when the satellite is at the horizon.

The vertical or zenith transmission is interesting because, in that case, there is no bending and, using the gas law and hydrostatic equation, it can be shown that, with a relatively good accuracy, the dry delay is proportional to the surface pressure while the wet zenith delay is proportional to the precipitable water PW:

$$PW = \frac{1}{\rho g} \times \int_{p_s} q_v dp$$

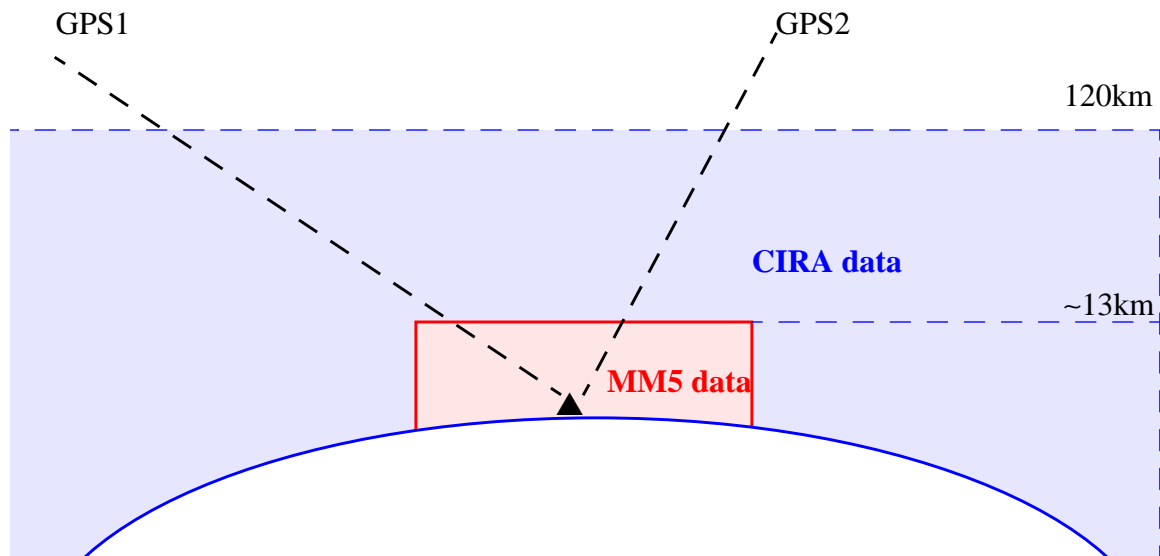
where ρ is the water density, \mathbf{g} the gravity acceleration, p_s the surface pressure, q_v the mixing ratio and p the pressure. As a rule of thumb, when expressed in the same unit, usually centimeters, the wet zenith delay is roughly 6.4 times the precipitable water. This direct relationship between the wet zenith delay and the precipitable water, and thus the mixing ratio, is very important since mixing ratio is usually the variable that characterizes moisture in NWP models. More challenging is the problem to extract moisture information in none necessarily zenith transmissions. Variational data assimilation is a possible approach and the modeling effort presented below is a step in that direction.

3.2 Ray-tracing

The ray-tracing code was adapted from the previous work of Zou *et al.* 1999. The changes mainly consist in the use of MM5 outputs instead of global data set and in the ray initialization procedure. Because the ray equation is a second order equation, two initial conditions, namely the initial position and initial direction, are required to begin the integration. While both the position of the GPS satellite and the position of the ground receiver at the time of transmission are observable and known with a good accuracy, the direction along which the ray has been emitted from the GPS is not observable. This direction depends on the properties of the slice of the atmosphere separating the satellite from the receiver. A perfect simulation that mimics the reality of the measurement would consist in ray-shooting. In ray-shooting, rays are initiated from the GPS satellite in various directions until one is found to reach the receiver. However, such approach is far too expensive and cannot be carried out. Instead we start the integration at the receiver in the direction of the straight line receiver-GPS. The resulting ray does not reach the GPS at its actual observed location, but the experiments show that the error is less than 100km at the GPS altitude (20 000km). Such difference is small and in any case has no impact in the phase since there is no neutral refractivity gradients at this height. Starting from the receiver also allows to better match the actual ray in the troposphere, that is, where the atmospheric refractivity gradients are most important. As said, the divergence of the two paths in the upper atmosphere has no impact as the refractivity gradient are almost absent up there.

An other problem is the limited domain aspect of the mesoscale model. To limit computational cost, high resolution simulations can only be performed on small domain around the receiver. Thus at low elevation angle, rays travel almost horizontally and rapidly exit from the model domain. Ideally, the ray tracing would start from the receiver using the highest resolution refractivity field of the smallest domain and as rays horizontally exit the domain, the

refractivity field of the next domain should be used and so on. Such interpolation procedure, however, requires to keep in the computer memory the three domains which is not possible in practice. Therefore, we had been using the CIRA climatological data from the COSPAR to compute the refractivity field outside the smallest domain. CIRA data consist in latitudinal monthly means of pressure and temperature given every 5km from 0 to 120km. These data were also used above the model lid (between 10km and 13km) so that we were able to perform the ray-tracing until neutral refractivity is null (around 60km). In practice, CIRA data are smooth at high elevation and the corresponding refractivity gradients are weak so that they have an almost negligible impact on the phase delay. Nonetheless, CIRA data allow for the computation of the full phase, which might be useful in the future. The sketch below illustrates the data configuration:



GPS positions were provided by JPL every five minutes for a maximum of 12 satellites simultaneously at a time. The 3-dimensional refractivity field was created at the transmission time by interpolation between two successive hourly 3.3 km resolution model outputs valid just before and just after the transmission time. Starting from the location of the receiver on the ground and the direction of the straight line receiver-satellite as initial direction, the ray is numerically integrated using a fourth order Runge Kutta method. At each step, the dry and wet refractivity and their vertical gradients are evaluated and the corresponding phase delay accumulated. One step is done in the direction of the gradient with a constant integration step of 100m within the MM5 domain and 5km in the CIRA data. Since we are using a 4th order Runge-

Kuntta method, this represents one point every 25m, which is less than the thinnest model sigma layer. So we are sure that there are, at least, one ray point per sigma level during vertical transmission. For low elevation angle, of course, the resolution of the ray-tracing is closer to the model horizontal resolution (3.3km) and an integration step of 25m is not needed but rather a computational burden. In the future, we will try to adjust the integration step as a function of the model vertical and horizontal resolution and the satellite elevation angle. To validate the code, we compared the precipitable water retrieved from ray-tracing in the zenith direction to precipitable water values computed independently using the hydrostatic assumption. Although no major differences were noted, ray-tracing seems to be prone to round-off error.

Ray-tracing is also computationally very demanding. It roughly takes two or three days of CPU time of one node of a DEC alpha machine ES40 to produce one day of GPS LOS observations (1 transmission every 5mn from up to 12 satellites). For that reason, it wasn't possible to perform the ray-tracing on-line, i.e. during the model integration. The interest to perform the ray-tracing in the model integration is that the refractivity field used is the one actually valid at the observation time. In our off-line approach, refractivity were saved every hour and linearly interpolated at the observation time. With this approach, we had been able to take advantage of the 8 nodes of the same DEC alpha machine. Satellite observations were gathered by batch of 3 hours and each batch was assigned to one of the 8 nodes. This technique has permitted to reduce the CPU time to less than 6 hour for one day of data.

Figure 4 shows the dry, wet and total delays as a function of the elevation angle for the entire day of July 17, 1999. This represents 2245 simulated transmissions. One can clearly see the variations of the phase delays which increase exponentially as elevations angle goes to 0. For low elevation angles, rays travels almost horizontally in the atmosphere and, therefore, stay longer in the troposphere were they are likely to encounter refractivity gradients.

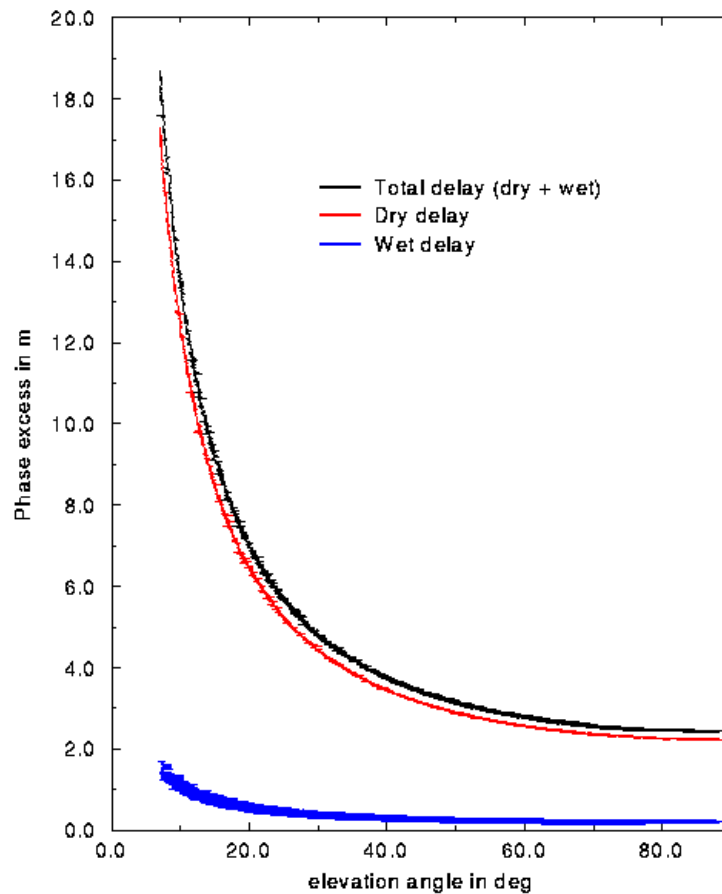


Figure 4:
 Dry (red), Wet (blue) and Total (black) phase delay (in meters)
 for all GPS transmissions available on July 17, 1999 (2245 transmissions)
 plotted as function of the satellite elevation angle (in degree).

Figure 5a shows the same delays as a function of the time for one satellite only (satellite 4). From the decrease and then increase of the delays we can deduce that the satellite firstly appeared rising to the ground receiver around 09z. The minimum of the curve shows that the zenith position was reached around 13z. Then the satellite was setting and completely disappeared from the receiver LOS at approximately 17z. Figure 5b shows the same plots for satellite 1. This satellite was at the zenith of the receiver at 02z and then disappeared from the receiver for most of the day.

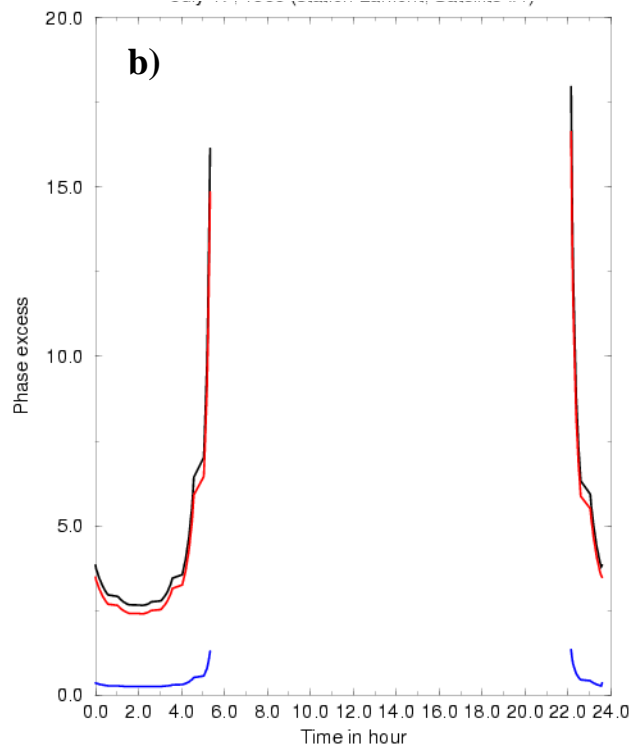
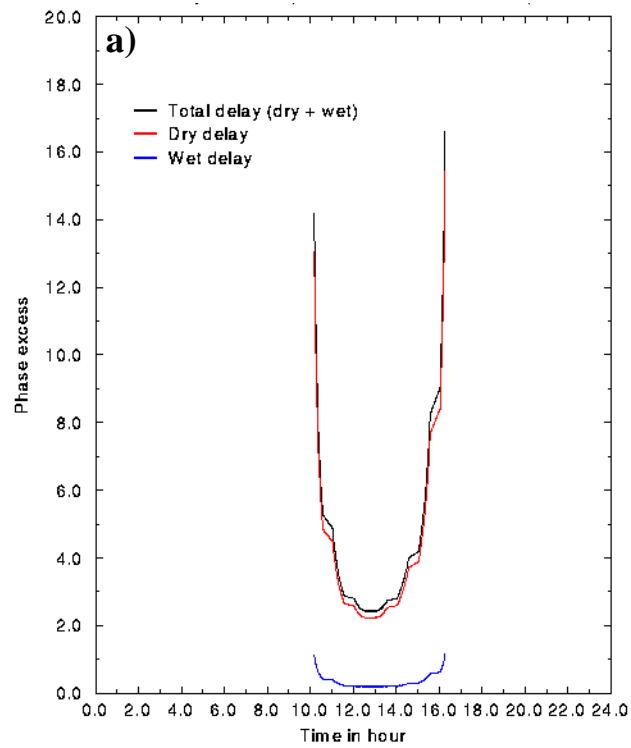


Figure 5:

Dry (red), Wet (blue) and Total (black) phase delay (in meters) for transmissions from GPS satellites #4 (a) and satellite #1 (b) available on July 17, 1999 plotted as function of time (in hour).

Model simulated LOS wet delays had been sent to JPL where they have been compared to the GPS and WV radiometers actual measurements. Figure 6 shows the GPS (red curve), the WV radiometer (green curve) wet zenith delays estimated from the LOS observations with the help of a Kalman filter and the model simulated wet LOS delays (blue curve) as a function of time for July 16 and 17, 1999. On this plot, there's only one GPS and WV radiometer datum at a given time (the projection on the zenith direction of the 12 LOS observations), while there are all the LOS data (up to 12) for the model curve. Despite, the plotted quantities are not exactly the same, we should expect a similar trend for the three curves. This is actually the case for the GPS and WVR, but not really for the model. The model curve is always below the other curves and exhibits important kinks at $t = 15.2$ (July 16 at 05z), $t=15.6$ (July 16 at 15z), $t=16.0$ (July 17 at 00z) and $t=16.6$ (July 17 at 17z). The kink on July 17, 00z can be attributed to the re-initialization of the model. The new analysis come from a separate source and differ from the model forecast. In particular, it seems that the analysis better matches the observations than the forecast. This is to be expected since the analysis contains new observational information while the forecast is still based on 12h old information. This may also an indication that at this resolution (3.3km) the predictability limit is certainly less than 12h. Note also, that same kink, although less important in magnitude, occurs between 15.5 and 15.6 and 16.4 and 15.6, which corresponds to the mid-day re-initialization of the model. For those re-initializations, however, the 12h forecast started at 00z, and not the analysis valid at 12z, was used to simulate LOS transmission occurring between 12z and 13z. In other words, LOS data between 12z and 13z were obtained by interpolation between the 12h forecast initiated at 00z and the 1h forecast initiated at 12z. This use of model output only and not analyzed fields seems to be provide more consistency in the data. Other kinks are unexplained and under investigation.

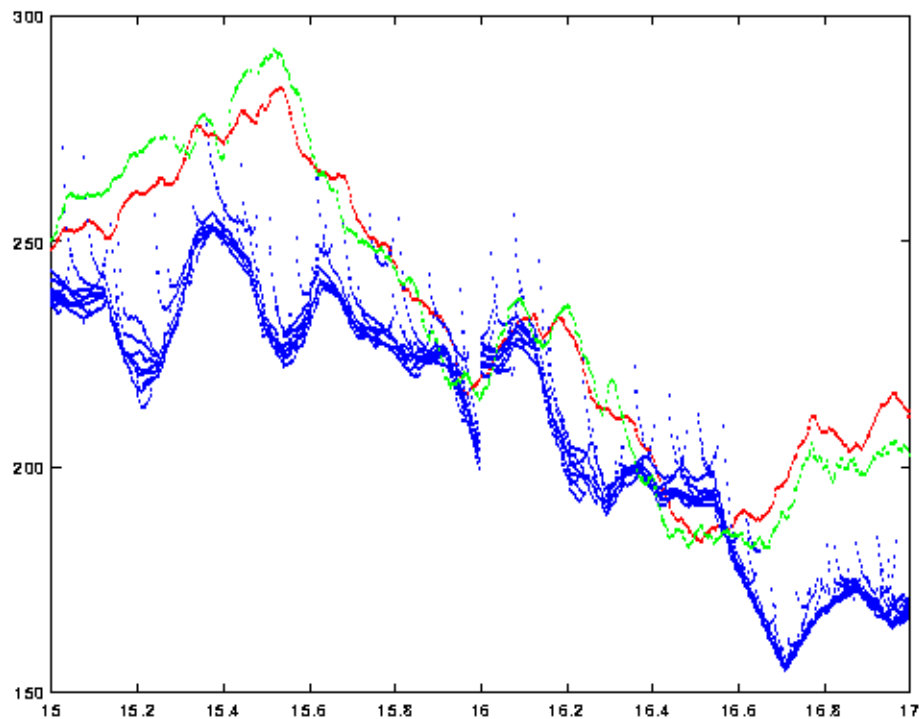


Figure 6:

GPS (red), the WV radiometer (green) and model simulated (blue) wet zenith delays
 The x-axis shows the day after July 1st, 1999, thus July 16 stands between 15 and 16,
 one mark represents a fifth of a day (4h 48mn).

An interesting feature is that the model curve is consistently under the observation curves, indicating that, in those simulation, the model systematically underestimates water vapor. This, undoubtedly, has to be related to the lack of local observations in the simulations. Because, no additional analyses were performed prior to the forecast, the 3.3 km model is initialized with data from global and continental observational networks, which do not resolve the scale involved in these high resolution simulations. In fact, the differences between the 30km and the 3.3km simulations are mainly due to topographic effects, which are certainly not enough to generate the moisture observed locally by both the GPS LOS receivers and WV radiometers. The inclusion in the model of local observations from the ARM data base will certainly help to reduce the differences between model simulated and observed GPS LOS. NCAR is presently collecting the observations and developing the software necessary to include these data in the initialization procedure.

4.0 Conclusion

A ray-tracing operator able to simulate GPS LOS observation with the fifth generation of the Penn State/NCAR mesoscale model has been developed and applied to simulate high spacial and temporal resolution GPS LOS data in a real configuration. Preliminary comparisons between model simulated and real observations indicate that GPS LOS observation contains lot of information on tropospheric moisture which are absent from continental observation networks. NCAR is currently working on the inclusion of local observations in the model initial conditions. Comparison between model simulated LOS transmission wet phase delay initialized with local information and actual GPS measurements will ultimately reveal the value of GPS LOS data for mesoscale data assimilation purposes.

5.0 Acknowledgements

The numerical simulations were performed on Compaq Alpha machines supplied under a joint External Technology Grant between Compaq, iMSC Corporation (www.imsc.com), and UCAR.

6.0 References

Haines, B.J. and Y. E. Bar-Sever: Monitoring TOPEX microwave radiometers with GPS: stability of columnar water vapor measurements. *Geophys. Res. Lett.*, 25, 3563-3566. 1998.

Bevis M. S., S. Businger, T. A. Herring, C. Rocken, R. A. Anthes and R. H. Ware: GPS meteorology: remote sensing of atmospheric water vapor using the global positioning System. *J. Geophys. Res. Atmosphere*, Vol 97, 15,797-15,801, 1992.

Grell A. G., J. Dudhia and D. R. Stauffer: *A description of the fifth-generation PennState/NCAR mesoscale modeling system*. Technical Note 938, National Center for Atmospheric Research, Boulder CO, 1994.

Kravtsov Y.A. and Y. I. Orlov: *Geometrical optics of inhomogeneous media*. 312 pp., Springer-Verlag, New-York, 1990.

Ware R., C. Alber, C. Rocken, F. Solheim: Sensing integrated water vapor along GPS ray paths. *Geophys. Res. Lett.*, 24, 417-420. 1997.

Rogers, E., D. Deaven, G. DiMego, 1995: The regional analysis system for the operational “early” eta model: original 80-km configuration and recent changes. *Weather and Forecasting*, 10(4): 810-825.

Zou X., F. Vandenberghe, B. Wang, M. E. Gorbunov, Y.-H. Kuo, S. Sokolovskiy, J. C. Chang, J. G. Sela and R. Anthes: A ray-tracing operator and its adjoint for the use of GPS/MET refraction angle measurements. *J. Geophys. Res.*, Vol 104, No D18, 22,301-22,318. September 1999.

Zumberge J.F., M. B.Heflin, D.C. Jefferson, M. M. Watkins and F. H. Webb: Precise point positioning for efficient and robust analysis of GPS data from large network. *J. Geophys. Res.*, Vol 102, No B3, 5005-5017. March 1997.